Mitteilung

Fachgruppe: Allgemeine Strömungstechnik

Reynolds number and humidity dependency of dropwise condensation in moist convective air flows

Andreas Westhoff[1], Konstantin Niehaus[1], Marie Volk[1] and Claus Wagner[1,2]

[1]Institute of Aerodynamics and Flow Technology, German Aerospace Center (DLR), Göttingen (Germany)
[2]Institute of Thermodynamics and Fluid Mechanics, Technische Universität Ilmenau, Ilmenau (Germany)

Condensation and evaporation on surfaces in moist convective air flows are phase transition phenomena that occur in many technical application or in nature. An example of condensation known from our everyday life is fogging of cold surfaces such as panes or glasses, where condensation usually occurs dropwise. The water droplets lead to a change in the optical properties, which can cause problems in situations where optical transparency is significant. For instance, condensation on vehicle windows, in headlamps, or on sensors leads to safety-relevant functional restrictions [1]. Moreover, due to the strong dipole moment of the water molecules condensation and evaporation have a significant influence on the heat transfer. For heat exchangers dropwise condensation is used to enhance the heat transfer performance [2]. Furthermore, defogging of a wind shield in an electronic vehicle requires a large amount of electric energy which results in a shorter driving range [3].
In such flows, as mentioned above, the process of phase transition and the convective flow is strongly influenced by the sensible and the latent heat transfer. Additionally, the droplet shape (contact angle), the surface properties and the spatial distribution of the droplets also have a strong influence. Hence, empirical models or numerical calculations often fail to predict the heat and mass transfer due to the large number of parameters and the mutual interplay of the different heat transport mechanisms. To obtain a reliable prediction of the mass and the heat transfer, time-consuming and cost-intensive experiments or computationally expensive numerical simulations are necessary. Neither is feasible in the development and design process for industrial applications. It would be too costly and time consuming. Therefore, the method of predicting the droplet size distribution and the corresponding heat transfer by means of a scalar model is of vital interest. To overcome this issue we have been developing a prediction model based on the scaling of system characteristic numbers. Part of this approach is to investigate the effect of large-scale flow structures on the dynamics of the droplet size distribution and the corresponding sensible heat transfer and the condensation mass transfer.

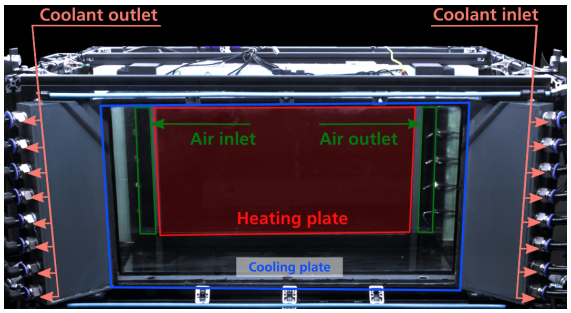

(a) photograph (front view)

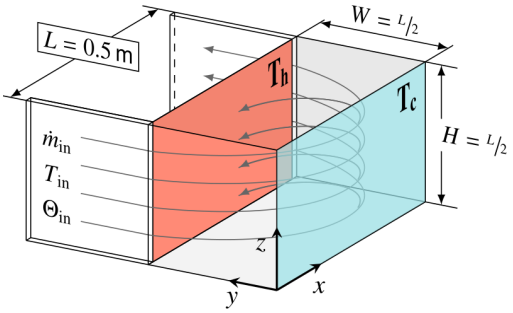

(b) sketch of the container and the air flow

Figure 1: Experimental set-up: (a) photograph of the configuration with: cold wall (front), warm wall (back), air inlet (left), and air outlet (right). (b) visualisation of the primary air flow with the corresponding boundary conditions for the isothermal side walls and at the air inlet.

Therefore, measurements of dropwise condensation on a cooled surface in moist convective air flows were performed. Figure 2 shows: a photo of the setup (figure 1a) and a sketch of the container geometry with a visualisation of the bulk air flow (figure 1b). The setup consists of a rectangular box with the dimensions: length $L = 0.5\,\mathrm{m}$, width $W = 0.5 \times L$, and height $H = 0.5 \times L$ with an isothermally cooled front wall and a heated rear wall. All other side walls are adiabatic. The forced flow is supplied

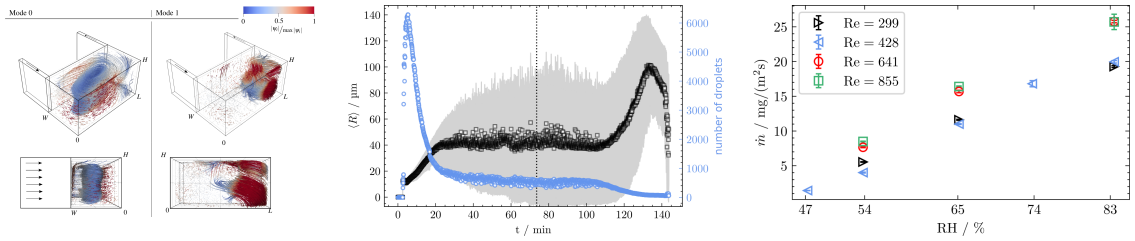

(a) coherent structures (b) particle size (c) mass flow

Figure 2: Topology of the first two POD modes revealing the predominant coherent flow structures. (b) Mean size and standard deviation of the particle size distribution and the corresponding number of droplets as a function of time for condensation and evaporation. (c) Mass flow of water due to phase transition as a function of time.

by an air inlet on the left and an outlet on the right side. Both slots span the full height and have a width of $W_{\text{slot}} = 0.05 \times L$. The inflow conditions are constant in terms of moist air mass flow $\dot{m}_{\text{in}}$, temperature $\dot{T}_{\text{in}}$ and dew point $\dot{\Theta}_{\text{in}}$. In order to measure the system relevant properties the setup is equipped with a plethora of temperature and humidity sensors. Furthermore, time-resolved velocity measurements for the three-dimensional flow field as well as optical measurements for the droplet size distribution on the cold surface were applied. Details of both measurement configurations can be found in Niehaus et al. [4] and Volk et al. [5].

Figure 1 depicts sample results of the flow and particle size measurements. With the objective to characterise the large-scale flow structures and to identify the influence of these structures on the heat and mass transfer an analysis of the velocity vector fields is performed by means of a proper orthonormal decomposition (POD). The topology from the POD calculation for the first two modes is imaged in figure 2a for $\mathcal{R}e = 254$, where the Reynolds number is defined as $\mathcal{R}e = \dot{m}_{\text{in}}/\nu H$ and ν is the dynamic viscosity. The mode $n = 0$ represents the dominant flow structure resulting from the forced convection. Air enters the container through the inlet follows the left wall, detaches, flows over the cold front, and detaches again. The flow then splits into two parts: one part leaves the container through the outlet and the other part flows along the heating plate, detaches and mixes with the air from the inlet. As a result, a large-scale circulation is developed in the bulk. Further, a second large-scale coherent structure is identified. Here, mode $n = 1$ is associated with the vortex located in the right front corner. These two structures have a significant impact on the vapour mass transfer $\dot{m}_v$ as well as on the particle size distribution, while the structure itself depends on $\mathcal{R}e$. Figure 2b shows the mean particle size (black squares) and the corresponding standard deviation (grey) of the particle size distribution for an evaluation area of $3.97\,\text{mm} \times 3.29\,\text{mm}$ for condensation (left of the dashed line) and evaporation (right side). Finally, figure 2c depicts the mass flow as a function of the relative humidity $RH = p_v/p_s$, where p_v and p_s denote the partial and the saturation vapour pressure, respectively. Here, the plot clearly reveals a scaling of the latent heat transfer and a $\mathcal{R}e$-dependency.

Based on these analyses, we will present a discussion on the scaling of sensible and latent heat transfer for dropwise condensation as a function of $\mathcal{R}e$ and RH. In addition, we will provide a brief introduction to the measurement techniques used.

[1] Matthias G Ehrnsperger, Uwe Siart, Michael Moosbühler, Emil Daporta, and Thomas F Eibert. Signal degradation through sediments on safety-critical radar sensors. *Advances in Radio Science*, 17:91–100, 2019.

[2] Dong Ho Nguyen and Ho Seon Ahn. A comprehensive review on micro/nanoscale surface modification techniques for heat transfer enhancement in heat exchanger. *International Journal of Heat and Mass Transfer*, 178:121601, 2021.

[3] Sun-Ik Na, Yoong Chung, and Min Soo Kim. Performance analysis of an electric vehicle heat pump system with a desiccant dehumidifier. *Energy Conversion and Management*, 236:114083, 2021.

[4] Konstantin A Niehaus, Andreas Westhoff, and Claus Wagner. Characterization of a mixed convection cell designed for phase transition studies in moist air. In *New Results in Numerical and Experimental Fluid Mechanics XIII: Contributions to the 22nd STAB/DGLR Symposium*, pages 483–493. Springer, 2021.

[5] Marie-Christine Volk, Konstantin A Niehaus, Andreas Westhoff, and Claus Wagner. Automated measurement of the number and growth of water droplets in mixed convection. In *23rd STAB/DGLR Symposium on New Results in Numerical and Experimental Fluid Mechanics*, 2022.